Chinese Journal of
POLYMER SCIENCE

ARTICLE

https://doi.org/10.1007/s10118-020-2392-z
Chinese J. Polym. Sci. **2020**, *38*, 898–907

Infusing High-density Polyethylene with Graphene-Zinc Oxide to Produce Antibacterial Nanocomposites with Improved Properties

You-Li Yao[a†], Manuel Reyes De Guzman[a†], Hong Duan[b], Chen Gao[a], Xu Lin[c], Yi-Hua Wen[a], Juan Du[a], Li Lin[a], Jui-Chin Chen[d], Chin-San Wu[e], Maw-Cherng Suen[f], Ya-Li Sun[a], Wei-Song Hung[g,h], and Chi-Hui Tsou[a,i,j*]

[a] *Material Corrosion and Protection Key Laboratory of Sichuan Province, Sichuan University of Science and Engineering, Zigong 643000, China*
[b] *Department of Orthopedics, West China School of Medicine/West China Hospital, Sichuan University, Chengdu 610041, China*
[c] *Department of Orthopedics, Fourth People's Hospital of Zigong, Zigong 643000, China*
[d] *Department of Materials and Textiles, Oriental Institute of Technology, New Taipei City 22061, China*
[e] *Department of Applied Cosmetology, Kao Yuan University, Kaohsiung 82101, China*
[f] *Department of Fashion Business Administration, Lee-Ming Institute of Technology, New Taipei City 24305, China*
[g] *Graduate Institute of Applied Science and Technology, Department of Materials Science and Engineering, National Taiwan University of Science and Technology, Taipei 10607, China*
[h] *R&D Center for Membrane Technology, Department of Chemical Engineering, Chung Yuan University, Chung-Li 32023, China*
[i] *Sichuan Zhixiangyi Technology Co., Ltd., Chengdu 610051, China*
[j] *Department of Materials Science, Chulalongkorn University, Bangkok 10330, Thailand*

Electronic Supplementary Information

Abstract Nanocomposites of high-density polyethylene (HDPE) modified with 0.2 phr graphene-zinc oxide (GN-ZnO) exhibited optimal mechanical properties and thermal stability. Two other nano-materials—GN and nano-ZnO—were also used to compare them with GN-ZnO. Increasing the content of GN-ZnO gradually enhanced the antibacterial and barrier properties, but the addition of 0.3 phr GN-ZnO led to agglomeration that caused defects in the nanocomposites. Herein, we investigated the antibacterial and barrier properties of HDPE nanocomposites infused with different nanoparticles (GN, ZnO, GN-ZnO) of varying concentrations. HDPE and the nanoparticles were melt-blended together in a Haake-Buchler Rheomixer to produce a new environment-friendly nano-material with improved physical and chemical properties. The following characterizations were conducted: tensile test, thermogravimetric analysis, morphology, differential scanning calorimetry, X-ray diffraction, antibacterial test, and oxygen and water vapor permeation test. The results showed that the crystallinity of HDPE was affected with the addition of GN-ZnO, and the nanocomposites had effective antibacterial capacity, strong mechanical properties, high thermal stability, and excellent barrier performance. This type of HDPE nanocomposites reinforced with GN-ZnO would be attractive for packaging industries.

Keywords High-density polyethylene; Zinc oxide; Nanocomposite material; Antibacterial properties; Barrier performance

Citation: Yao, Y. L.; De Guzman, M. R.; Duan, H.; Gao, C.; Lin, X.; Wen, Y. H.; Du, J.; Lin, L.; Chen, J. C.; Wu, C, S,; Suen, M. C.; Sun, Y. L.; Hung, W. S.; Tsou, C. H. Infusing high-density polyethylene with graphene-zinc oxide to produce antibacterial nanocomposites with improved properties. *Chinese J. Polym. Sci*. **2020**, *38*, 898–907.

INTRODUCTION

Polymers are widely used in the beverage and food packaging industries because of their low density, low cost, substantial chemical inertness, and easy processability.[1–3] One of the most important requirements for packaging is high barrier performance. Plastics with excellent barrier properties are used in industrial applications that process materials which include medical and pharmaceutical products, electronic gadgets, and chemicals.[4–6]

Polyolefins (*e.g.*, polyethylene (PE) and polypropylene) are one type of the most widely used polymers in many fields including food packaging industries, agricultural firms, water piping, and tank-container storage.[7–10] As a polymer matrix, high-density PE (HDPE) exhibits strong mechanical properties, and it has a combination of attractive features such as low production cost and high resistance to thermal deformation.[11]

Nanocomposites consist of a polymer matrix and an organic or inorganic filler in the nanometer scale (1–100 nm).[12,13] At present, improvements in the properties of polymers (PE or HDPE, among others) are beneficial to numerous applications. The integration of nano-fillers into polymers has attrac-

* Corresponding author, E-mail: mayko0301@hotmail.com
† These authors contributed equally to this work.
Received September 25, 2019; Accepted January 17, 2020; Published online May 9, 2020

ted substantial interests.

Graphene (GN) was isolated in the mid-20th century.[14] Since then, polymeric nanocomposites containing GN and GN derivatives have been the subject of intense investigations. The reason is that they exhibit excellent electrical properties and thermal conductivity, as well as high aspect ratio.[15–17] Nanocomposites of polar polymers with GN and its derivatives have been widely studied. Examples of these polymers are as follows: poly(methyl methacrylate),[18,19] poly(vinyl alcohol),[20,21] poly(vinyl chloride),[22,23] and poly(ethylene terephthalate).[24,25]

Few studies have been conducted on the addition of GN or a derivative of GN to nonpolar polyolefins such as polystyrene[26] and polypropylene,[27–29] because dispersing it in melt-blended nonpolar polymers is a major challenge—nano-sheets have thermodynamic tendencies to form aggregates.[30] Because of the agglomeration, the interfacial adhesion in nonpolar polymers is poor (unlike in the case of polar polymers). Therefore, the modification of GN is an essential strategy to effectively mix GN with polyolefins.

Nanoparticles of metal oxides have high surface energies, small sizes, large surface atomic ratios, and large specific surface areas.[31,32] For these reasons, they have been widely used in several fields such as photocatalysis,[33] sunscreen cosmetics,[34,35] antibacterial materials,[36] and solar batteries.[37]

Zinc oxide (ZnO) is an n-type semiconductor with a band gap of 3.37 eV. The free exciton binding energy of ZnO at room temperature is greater than 60 MeV.[38,39] Its special photoelectric properties make it one of the most important semiconductors in the field of visible light bacteriostasis and photocatalytic deoxidation.[40,41] When the size of ZnO is reduced to a nanometer level, it can adsorb bacteria on its surface and inhibit the growth of most bacteria or even kill them.[42] This activity is largely attributed to the excellent hydrophobicity and oxidation capacity and high specific surface area of ZnO.[43]

Introducing additives (cross-linking agents) and inorganic fillers (GN, carbon nanotubes, ZnO) to PE or HDPE can improve the properties and performance of the polymer.[44–46] GN can effectively reinforce the polymer, but it is a weak antibacterial agent; thus, using it as a filler, especially in small amounts, would impart little or no antibacterial properties. On the other hand, nano-ZnO has an excellent antibacterial capacity, albeit its poor reinforcement ability. Combining the advantages of these two nano-materials would therefore make an effective nano-filler in the form of complexes of GN-ZnO.

The addition of GN-ZnO to HDPE produced a new nanocomposite (GN-ZnO/HDPE), which should supersede the original materials. Physical methods were used to infuse the conductive filler into the polymer. GN-ZnO/HDPE had advantages in terms of physical and chemical properties and synergistic effects, and it had antibacterial and conductive properties.

To evaluate the efficiency of the new nano-filler (GN-ZnO), it was compared with GN as a single filler, as well as with nano-ZnO alone. The mechanical properties, thermal stability, and antibacterial capacity of GN/HDPE, ZnO/HDPE, and GN-ZnO/HDPE were examined. The HDPE nanocomposites would have potential applications as packaging materials because of improved tensile and barrier properties, crystallinity, and antimicrobial activity.

EXPERIMENTAL

Materials

HDPE, known for its suitability in food packaging, was supplied by China Petroleum and Chemical Corporation. It was in a white granular form, with a density of 0.955 g·cm^{-3}. GN-ZnO (a specially-tailored new nano-filler) was custom-made by Apex Nano Co., Ltd. (New Taipei City, Taiwan Province, China). The ratio of GN to ZnO was roughly 1:2, which was evaluated using energy-dispersive X-ray spectroscopy (EDS) (Fig. S1 and Table S1 in the electronic supplementary information, ESI). Fig. S2 (in ESI) illustrates the morphology of GN-ZnO, showing ZnO nanoparticles in the form of flakes coating GN. The diameter of ZnO was 300–400 nm, and its thickness was 20 nm.

Preparation of Nanocomposites

A Haake-Buchler Rheomixer (Type 600), with a volume of 69 cm^3, was used to blend HDPE with different nanoparticles of varying concentrations (0.1, 0.2, and 0.3 phr) at 170 °C and 120 r·min^{-1} for 5 min to produce nanocomposites. The following nano-fillers were considered: GN, ZnO, and GN-ZnO. The melting temperature and torque were recorded by a computer. Nanocomposites of HDPE with 0.1, 0.2, and 0.3 phr GN-ZnO were designated as 0.1phrGN-ZnO/HDPE, 0.2phrGN-ZnO/HDPE, and 0.3phrGN-ZnO/HDPE, respectively.

Characterization

Mechanical testing

The mechanical properties of all samples were determined with the use of an FBS10KNW electronic universal testing machine (Xiamen Forbes Tensile Equipment Co., Ltd., China) operated at a speed of 50 mm·min^{-1}, according to the GB/T1040-2006 standard for testing the tensile strength of plastics. At least 5 samples were measured, and the obtained data were averaged. The total length of the dumbbell-shaped tensile samples was 115 mm, and the tensile section had the following dimensions: length, 30 mm; width, 4.3 mm; thickness, 1.4 mm. The load was applied along the axial direction until the sample broke. Tensile strength was measured at a certain test temperature and humidity.

Thermal gravimetry

A thermal gravimetric analyzer (Model HTG-1, Beijing Hengjiu Experimental Equipment Co., Ltd., China) was employed to evaluate the decomposition behavior of the samples. The heating rate was set equal to 10 °C min^{-1}. Heating was started from room temperature, and was stopped when the temperature reached 750 °C. Origin software was run to obtain a diagram of differential thermal gravimetry (DTG) for the tested samples (a plot of temperature versus rate of weight loss).

Field emission scanning electron microscopy-energy-dispersive X-ray spectroscopy

The morphology and elemental surface analysis of the HDPE nanocomposites were characterized using field emission scanning electron microscopy-EDS (FESEM-EDS, MIRA3 FEG-

https://doi.org/10.1007/s10118-020-2392-z

SEM, Tescan, Czech). Before the samples were examined, they were sputtered with gold dust to make them conductive.

In EDS, the characteristic X-ray energy emitted by different elements is unique, and the unique energy for Zn was the basis for determining its dispersion in the nanocomposites.

Differential scanning calorimetry

Data on the crystallization and melting temperatures, as well as the crystallization and melting enthalpies of the nanocomposites were recorded through differential scanning calorimetry (DSC, 200F3, Netzsch, Germany). At a rate of 10 °C·min^{-1}, heating was begun from room temperature to 180 °C. Then, the temperature was held at 180 °C for 3 min. Afterward, cooling was applied from 180 °C down to room temperature at a rate of 10 °C·min^{-1}. Samples and reference materials were separately placed in two crucibles, and they were heated at the same rate of 10 °C·min^{-1}. To eliminate the influence of previous thermal history of the samples, heating and cooling were conducted twice.

X-ray diffraction

The degree of crystallinity of the nanocomposites was investigated using X-ray diffraction (XRD, D8 Advance, Bruker, Germany) equipped with monochromatic Cu-Kα radiation (λ = 0.154 nm) under a voltage of 40 kV and a current of 40 mA. All samples were analyzed in continuous scan mode, with 2θ ranging from 5° to 90°.

Antibacterial test

The antimicrobial properties of GN/HDPE, ZnO/HDPE, and GN-ZnO/HDPE were tested on *Escherichia coli*. A qualitative analysis was performed. The main steps were as follows.

(1) Solid medium configuration. Beef paste peptone was sterilized at a high temperature and pressure in a kettle at 121 °C for 1 h. Then, the liquid was poured into a disposable Petri dish to a height one-third of the dish.

(2) Inoculation with *E. coli*. *E. coli* was used to activate the liquid medium (activation took 24 h). The culture medium was cooled and placed in an ultraviolet incubator. *E. coli* was inoculated with beef paste peptone through a dilution-coating method, and it was placed in a constant temperature and humidity incubator set at 37 °C and 30% humidity.

(3) Gathering of experimental results. After the bacterial culture that lasted for 24 h, bacteriostasis in the Petri dish was observed, and experimental data were recorded.

Water vapor transmission tester

To measure the water vapor permeability, a transmission tester (Labthink W3/060, Jinan, China) was used. The test environment temperature and humidity were controlled. As such, a fixed humidity difference was attained across the sample. The water vapor passed through the sample toward the dry side. Hence, the moisture was reduced, and the weight of the sample cup decreased. Analysis of the sample was conducted to determine the water vapor permeability and the permeability coefficient. The test interval was 30 min, with the temperature set at 25 °C and the humidity maintained at 90%.

Oxygen permeameter

Pretreated samples were sandwiched between the upper and the lower test chambers of a differential pressure gas permeameter (Labthink VAC-V2, Jinan, China). First, the low-vacuum chamber was emptied. Then, the high-pressure chamber was filled with oxygen at a certain pressure. Thus, the gas permeated from the high-pressure chamber to the low-pressure chamber under the action of a pressure difference. The permeability coefficient of the tested sample was obtained by measuring the lateral pressure at a low pressure. Degassing time in the chamber was 5 h. The operating temperature was controlled at 23 °C, with the humidity set at 50%.

RESULTS AND DISCUSSION

Mechanical Properties

Table 1 presents a comparison of the mechanical properties of HDPE modified with different nanoparticles (GN, ZnO, and GN-ZnO). Nanocomposites even with a low content of 0.1 phr GN indicated improvement in the properties, relative to neat HDPE, signifying that GN had a reinforcing effect. By contrast, HDPE filled with only ZnO (at all concentrations of 0.1, 0.2, and 0.3 phr) exhibited inferior tensile strength and elongation at break, demonstrating that ZnO effected no reinforcement because it failed to bind with the nonpolar HDPE.[47]

Table 1 Tensile strength and elongation at break of neat HDPE and its nanocomposites consisting of different nano-fillers of varying concentrations (parts per hundreds of resin, phr).

Nano-filler content (phr)	0	0.1	0.2	0.3
Tensile strength (MPa)				
HDPE	27.33	–	–	–
GN/HDPE	–	29.97	29.75	25.5
ZnO/HDPE	–	25.68	25.38	24.47
GN-ZnO/HDPE	–	28.00	30.00	29.67
Elongation at break (%)				
HDPE	32.4	–	–	–
GN/HDPE	–	41.75	24.07	18.67
ZnO/HDPE	–	20.68	18.46	25.25
GN-ZnO/HDPE	–	33.95	52.43	50.26

A combination of GN and ZnO as GN-ZnO nano-fillers also made HDPE tougher. For example, the HDPE nanocomposite with 0.2 phr GN-ZnO yielded a tensile strength that was 10% higher than that of neat HDPE, and an elongation at break that was 62% higher. However, adding 0.3 phr GN-ZnO reduced the mechanical properties; hence, 0.2 phr GN-ZnO could be considered the optimum content. A high concentration of the nano-filler would cause agglomeration, leading to defects in the nanocomposite.

The superiority of GN-ZnO/HDPE over the other two nanocomposites can be better visualized in Fig. 1. For each nanocomposite, the trend of data on tensile strength (Fig. 1a) was consistent with that on elongation at break (Fig. 1b). A peak occurred at 0.2 phr GN-ZnO (*i.e.*, the mechanical properties were optimal). The tensile strength peaked at 30 MPa, whereas the elongation at break peaked at 52.43%. For the case of 0.3 phr GN-ZnO, the dip in tensile strength or elongation at break might be due to defects because of the agglomeration.

Thermal Decomposition Temperatures

Fig. 2 illustrates the DTG curves for HDPE modified with different nano-fillers of varying concentrations (inset shows magnified peaks). DTG is the first-order differential weight loss with respect

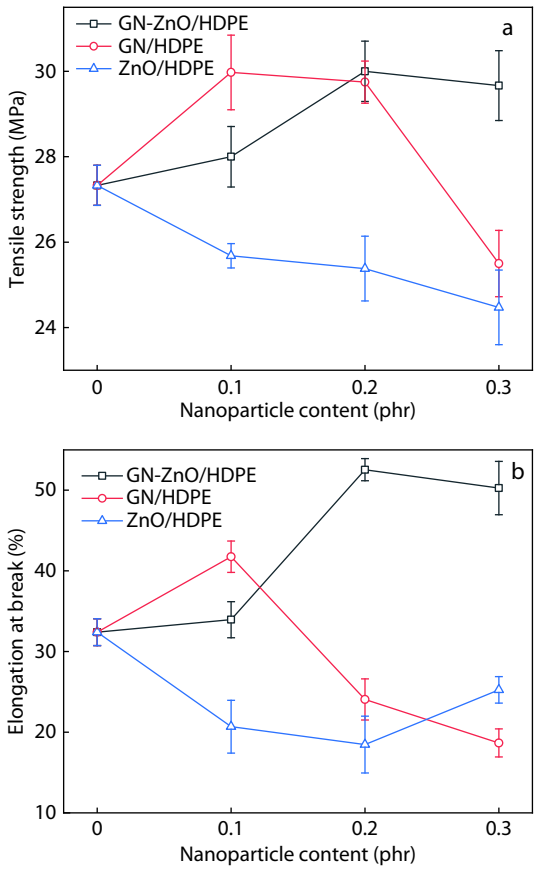

Fig. 1 Mechanical properties of GN/HDPE, ZnO/HDPE, and GN-ZnO/HDPE: (a) tensile strength; (b) elongation at break.

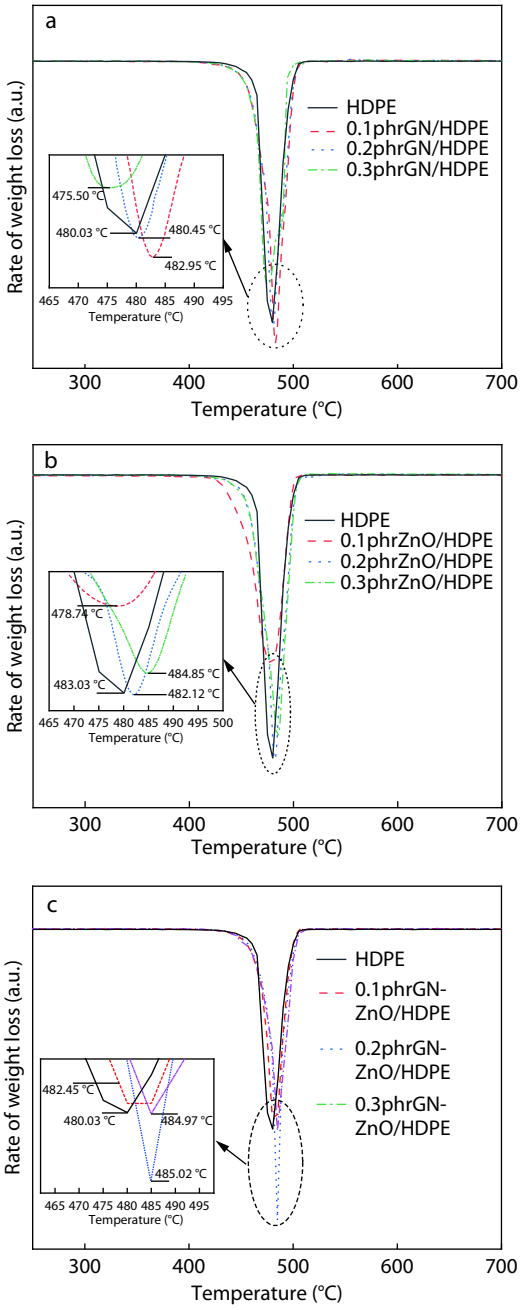

Fig. 2 Differential thermal gravimetric analysis of neat HDPE and modified HDPE containing different nanoparticles of various concentrations: (a) GN/HDPE; (b) ZnO/HDPE; (c) GN-ZnO/HDPE.

to temperature or time. The lowest peak is associated with the fastest rate of weight loss, and a peak corresponds to the decomposition temperature. HDPE had the lowest thermal decomposition temperature (480.0 °C).

The thermal degradation temperatures of GN/HDPE nanocomposites were 483.0, 480.5, and 475.5 °C when the content of GN was 0.1, 0.2, and 0.3 phr, respectively. If ZnO replaced GN as the nano-material present in the nanocomposites, the corresponding thermal degradation temperatures were 478.7, 482.1, and 484.9 °C.

In the case of GN-ZnO as the nano-filler, varying its content from 0.1 phr to 0.3 phr contributed to a consistent increase in the thermal decomposition temperature relative to that of neat HDPE. The inset demonstrates that the thermal decomposition temperatures were 482.5, 485.0, and 485.0 °C at 0.1, 0.2, and 0.3 phr GN-ZnO, respectively.

In summary, our specially-tailored new nano-filler (GN-ZnO) effected the greatest improvement in the thermal stability of HDPE, indicating its advantage over the single nano-materials (GN and ZnO).

Morphology

Fig. 3 illustrates the FESEM images of fractured surfaces of neat HDPE and GN-ZnO/HDPE nanocomposites. The surface of HDPE resembled untangled vertical threads of fiber (Fig. 3a). Modifying HDPE by blending it with even a small amount of GN-ZnO drastically changed its morphology to that of a dense structure.

In Fig. 3(b), 0.1 phr GN-ZnO apparently cemented the loose fibers of HDPE. The nanocomposite morphology became denser with the addition of 0.2 phr GN-ZnO (Fig. 3c). However, the presence of a greater amount of GN-ZnO (0.3 phr) led to agglomeration (Fig. 3d).

EDS was used to analyze the distribution of Zn in GN-ZnO/HDPE nanocomposites, as a way of demonstrating the dispersion of the nano-fillers. FESEM images are given by Figs. 4(a)–4(d), whereas EDS images are those in Figs. 4(a′)–4(d′). Fig. 4(a) depicts the surface FESEM image of neat HDPE,

https://doi.org/10.1007/s10118-020-2392-z

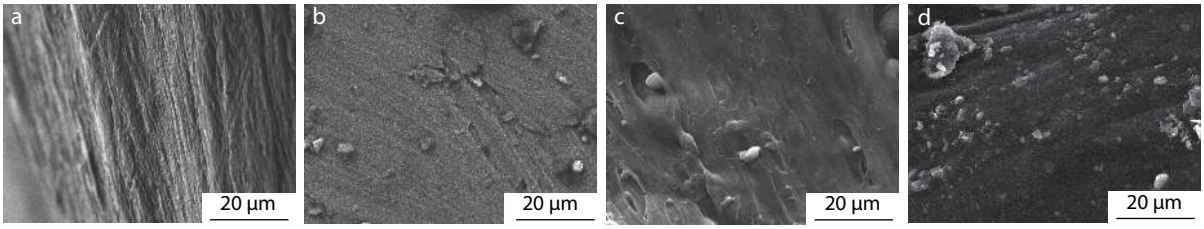

Fig. 3 FESEM images of fractured surfaces: (a) HDPE; (b) 0.1phrGN-ZnO/HDPE; (c) 0.2phrGN-ZnO/HDPE; (d) 0.3phrGN-ZnO/HDPE.

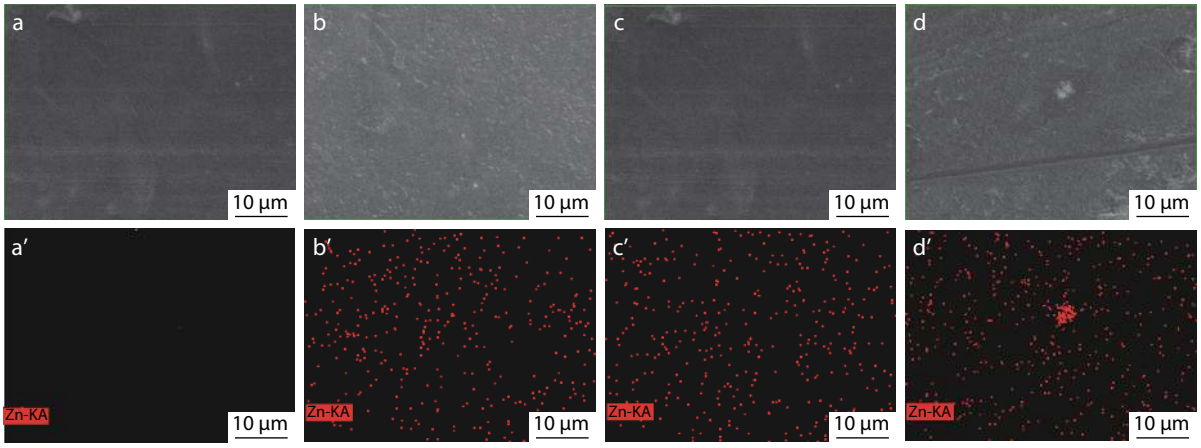

Fig. 4 (a–d) Surface FESEM images and (a′–d′) surface EDS images illustrating the distribution of Zn: (a, a′) HDPE; (b, b′) 0.1phrGN-ZnO/HDPE; (c, c′) 0.2phrGN-ZnO/HDPE; (d, d′) 0.3phrGN-ZnO/HDPE.

which was unfilled with GN-ZnO; therefore, no Zn was detected in the EDS image (Fig. 4a′). Zn was uniformly dispersed in the nanocomposites when the concentrations of GN-ZnO were 0.1 phr (Fig. 4b′) and 0.2 phr (Fig. 4c′). However, when the content of GN-ZnO increased to 0.3 phr, agglomeration occurred (Fig. 4d′).

Differential Scanning Calorimetry Data

The data in Table 2 (obtained from Fig. 5) show that the melting point of each GN-ZnO/HDPE nanocomposite was lower than that of neat HDPE, because GN-ZnO promoted nucleation (or the generation of a higher number of crystal core). Enhanced nucleation hindered crystallization; thus, crystallization temperatures were higher. A slower crystallization rate caused HDPE to melt at a lower temperature in the heating process.

From Table 2, the melting enthalpy of either 0.1phrGN-ZnO/HDPE (210.7 J g^{-1}) or 0.2phrGN-ZnO/HDPE (194.5 J·g^{-1}) differed little from that of neat HDPE (200.4 J·g^{-1}). By contrast, the melting enthalpy of 0.3phrGN-ZnO/HDPE was considerably lower (113.3 J·g^{-1}). Therefore, a greater amount of GN-ZnO (0.3 phr) caused structural defects in the nanocomposite because of the additive agglomeration, resulting in poor thermal properties and stability.

Degree of Crystallinity

XRD patterns of GN-ZnO, neat HDPE, and GN-ZnO/HDPE nanocomposites (Fig. 6) indicate peaks corresponding to the following crystallinity data (Table 3): HDPE, 73%; 0.1phrGN-ZnO/HDPE, 70.9%; 0.2phrGN-ZnO/HDPE, 70.4%; 0.3phrGN-ZnO/HDPE, 71.6%. Adding GN-ZnO to HDPE affected the crystallinity to an extent. In the case of 0.2 phr GN-ZnO, the nanocomposite crystallinity was lower by 2.6%, relative to that of HDPE. For 0.3 phr GN-ZnO, the crystallinity was also lower, but only by 1.4%. In other words, adding a greater amount of GN-ZnO (0.3 phr) produced a nanocomposite that approached the rigidity and crystallinity of neat HDPE.

According to Fig. 6 and Table 3, GN-ZnO registered only one characteristic peak at 11.06°, and the characteristic peaks of HDPE were 21.23°, and 23.51°. With the addition of GN-ZnO, shifts in the characteristic peaks of the resultant nanocomposites were only small, and the characteristic peak of ZnO was not observed. A probable reason is that only small amounts of GN-ZnO were added, so the presence of ZnO could not be detected.

Table 2 Data on melting and crystallization temperatures and on melting and crystallization enthalpies.

Sample	The first melting		The first crystallization		The second melting		The second crystallization	
	Temperature (°C)	Enthalpy (J·g^{-1})	Temperature (°C)	Enthalpy (J·g^{-1})	Temperature (°C)	Enthalpy (J·g^{-1})	Temperature (°C)	Enthalpy (J·g^{-1})
HDPE	143.4	170.9	120.0	190.0	139.8	200.4	120.0	186.5
0.1phrGN-ZnO/HPDE	139.4	194.3	120.9	179.2	135.9	210.7	121.0	196.2
0.2phrGN-ZnO/HPDE	141.2	202.6	121.2	192.1	138.3	194.5	121.2	186.5
0.3phrGN-ZnO/HPDE	138.2	115.2	121.5	96.63	134.9	113.3	121.5	103.4

https://doi.org/10.1007/s10118-020-2392-z

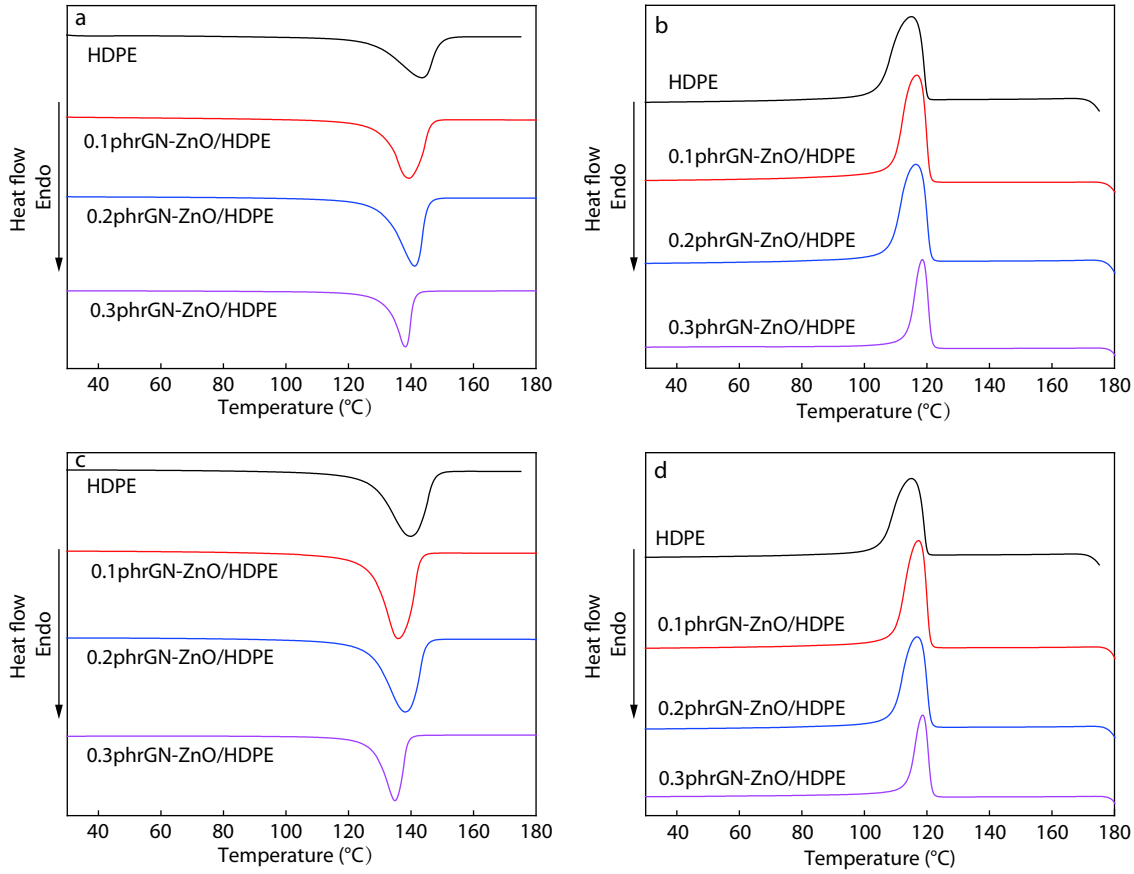

Fig. 5 Differential scanning calorimetry for HDPE and GN-ZnO/HDPE nanocomposites: (a) the first heating curves; (b) the first cooling curves; (c) the second heating curves; (d) the second cooling curves.

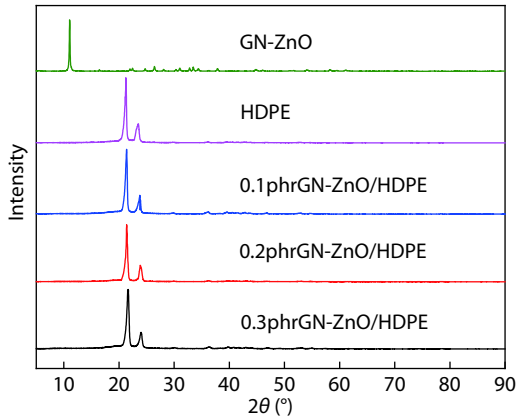

Fig. 6 X-ray diffraction patterns of HDPE, GN-ZnO, and GN-ZnO/HDPE nanocomposites.

Antimicrobial Activity

Fig. 7 shows images of *E. coli* colonies in each dish, arranged in rows and columns. HDPE nanocomposites containing different nano-fillers, namely GN, ZnO, and GN-ZnO, were aligned in the first, second, and third rows, respectively.

The samples were grouped in four columns according to the nano-filler content (0, 0.1, 0.2, 0.3 phr): the first column, HDPE; the second column, 0.1phr(nano-filler)/HDPE; the third column, 0.2phr-(nano-filler)/HDPE; the fourth column, 0.3phr (nano-filler)/HDPE.

In the middle of each dish was the sample with a round shape. HDPE by itself and GN/HDPE nanocomposites had no antibacterial effect. However, the nanocomposites containing ZnO and GN-ZnO had effective inhibitory action on the growth of *E. coli*. Higher amounts of ZnO and GN-ZnO had more effective antibacterial effects, as indicated by the growing dimension of inhibition area around the sample. Because of the strong photocatalytic ability of ZnO, it exhibited greater antibacterial activity than GN-ZnO.

Table 3 Crystallinity and characteristic peaks, as measured by X-ray diffraction.

Sample	Degree of crystallinity (%)	Characteristic peaks at 2θ (°)	
GN-ZnO	82.7	11.06	
HDPE	73.0	21.23	23.51
0.1phrGN-ZnO/HDPE	70.9	21.31	23.77
0.2phrGN-ZnO/HDPE	70.4	21.40	23.86
0.3phrGN-ZnO/HDPE	71.6	21.58	23.94

Water Vapor Permeability

Fig. 8 plots data on instantaneous (Fig. 8a) and average (Fig. 8b) water vapor permeability coefficients for HDPE and its nanocomposites. Fig. 8(b) indicates a peak at 0.1 phr content of GN-ZnO. A higher content led to a decrease in the permeability coefficient, the lowest being at 0.3 phr GN-ZnO. The average

https://doi.org/10.1007/s10118-020-2392-z

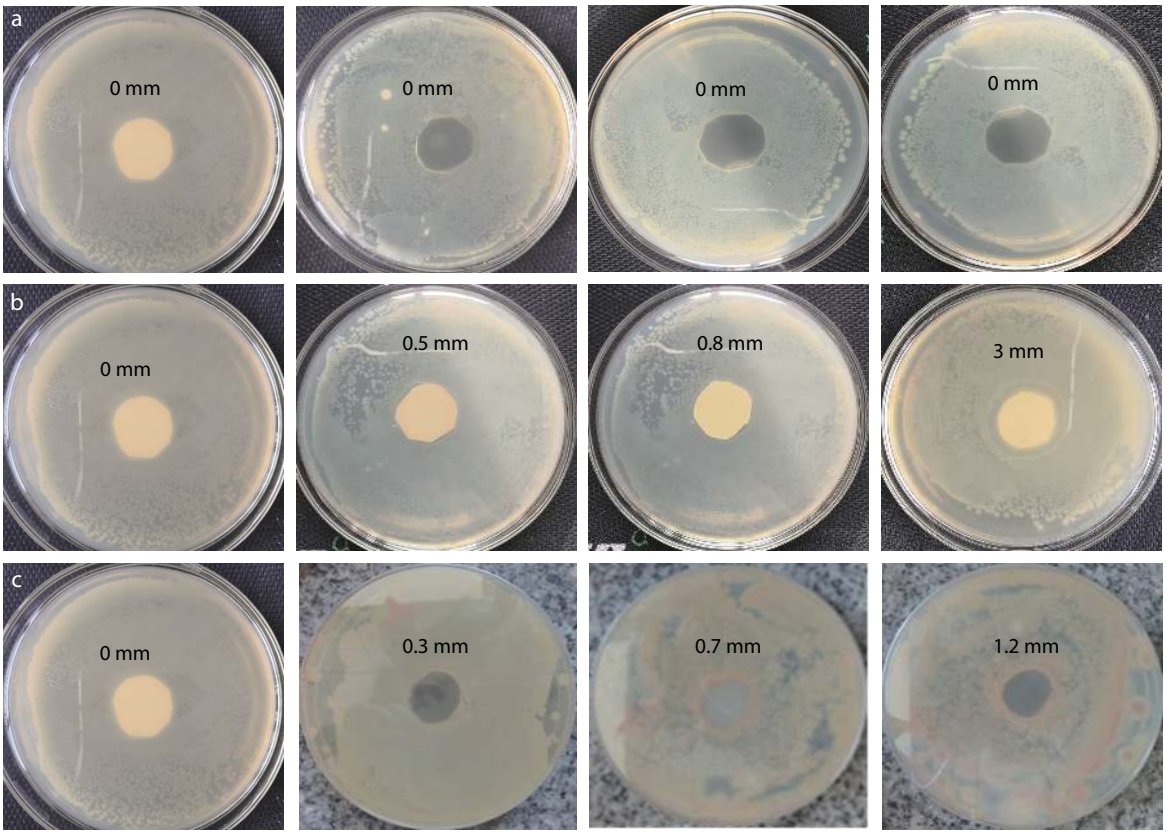

Fig. 7 Inhibition effect of HDPE and its nanocomposites containing different nano-fillers of varying concentrations on growth of *Escherichia coli*: (a) GN/HDPE; (b) ZnO/HDPE; (c) GN-ZnO/HDPE.

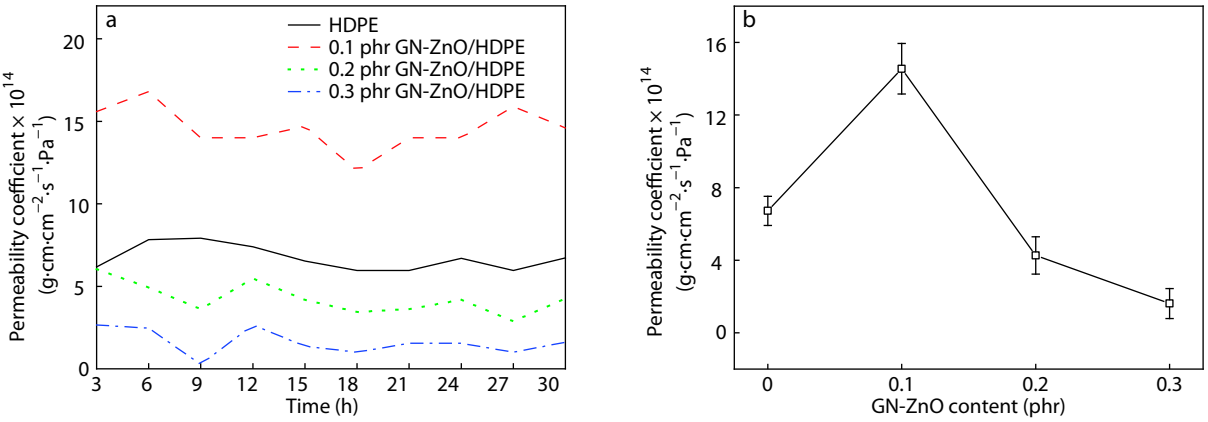

Fig. 8 (a) Instantaneous and (b) average water permeability coefficients for HDPE and GN-ZnO/HDPE nanocomposites.

water vapor permeability coefficient (g·cm·cm^{-2}·s^{-1}·Pa^{-1}) was 6.71 × 10^{-14} for HDPE, 1.46 × 10^{-13} for 0.1phrGN-ZnO/HDPE, 4.26 × 10^{-14} for 0.2phrGN-ZnO/HDPE, and 1.61 × 10^{-14} for 0.3phrGN-ZnO/HDPE.

The downward trend of data for the nanocomposites (Fig. 8b) might be attributed to the hydrophobicity of the polyolefin HDPE polymer and its lack of functional groups. As such, ZnO did not readily bind with HDPE, and interfacial defects were formed between HDPE and GN-ZnO. However, the nanocomposites were much less permeable than neat HDPE.

The permeability of 0.2phrGN-ZnO/HDPE was lower than that of neat HDPE, which may be due to the dispersion of GN in HDPE.

Fig. 9 depicts that the presence of GN-ZnO lengthened the path of water vapor permeation and enhanced the barrier performance of the nanocomposite.

Oxygen Permeability

The effect of filling HDPE with GN-ZnO was to lower the oxygen transmission coefficient (Fig. 10). The lowest transmission coefficient was when 0.2 phr GN-ZnO was added to HDPE. However, the addition of 0.3 phr GN-ZnO led to an increased transmission coefficient of oxygen. The reason is the agglome-

https://doi.org/10.1007/s10118-020-2392-z

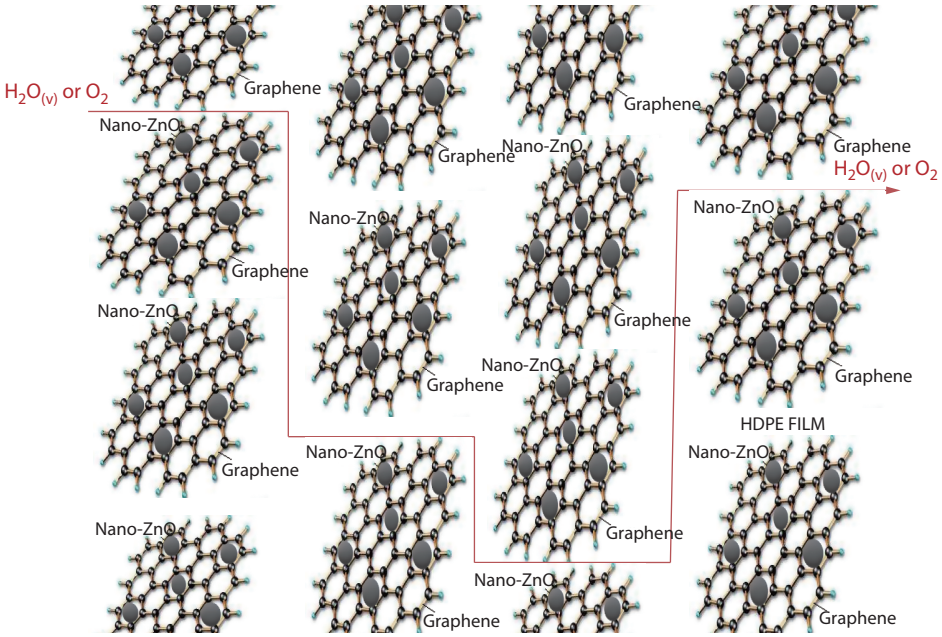

Fig. 9 Schematic of molecular permeation path for water vapor.

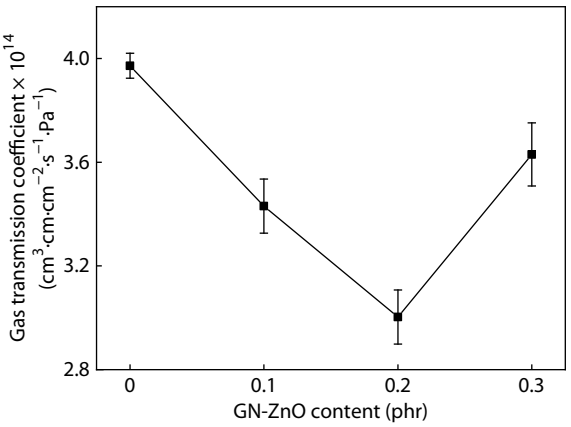

Fig. 10 Oxygen transmission coefficients for HDPE and its nanocomposites.

ration of GN at this high content of GN-ZnO. Hence, the pathway for the passage of oxygen was shorter. Nonetheless, the coefficient was still lower than that for neat HDPE.

CONCLUSIONS

In this present study, HDPE was selected as the polymer matrix and GN-ZnO as an additive or a filler for modifying HDPE. The obtained nanocomposites were examined in terms of the following parameters: mechanical properties, morphology, thermogravimetric data, crystallinity, antimicrobial activities, and barrier performance. The results are summarized as follows:

(1) The tensile strength and elongation at break of the nanocomposites were considerably improved when 0.2 phr GN-ZnO was added, but increasing the concentration further to 0.3 phr led to the reduction of the mechanical properties. At this higher concentration, FESEM images showed the incompatibility between HDPE and GN-ZnO.

(2) The thermal decomposition temperature of HDPE gradually increased with the addition of GN-ZnO. Hence, filling HDPE with certain amounts of GN-ZnO improved the thermal stability of the nanocomposites.

(3) The crystallinity of HDPE decreased when GN-ZnO was incorporated, which may be caused by the incomplete crystallization of the HDPE nanocomposites.

(4) Nanocomposites of HDPE containing different nanoparticles (GN, ZnO, GN-ZnO) exhibited different degrees of inhibitory effects on the growth of *E. coli*. The addition of GN did not show any antibacterial property, but modifying HDPE with ZnO and GN-ZnO produced an effect. The antibacterial activity of ZnO/HDPE was stronger than that of GN-ZnO/HDPE. Adding a higher content of GN-ZnO demonstrated superior bacterial inhibition.

(5) The addition of GN-ZnO could reduce the water vapor and oxygen permeability and enhance the barrier performance of the nanocomposites.

Electronic Supplementary Information

Electronic supplementary information (ESI) is available free of charge in the online version of this article at https://doi.org/10.1007/s10118-020-2392-z.

ACKNOWLEDGMENTS

The authors would like to acknowledge the financial support from the following organizations: Wuliangye Group Co., Ltd. (No. CXY2019ZR001); Sichuan Province Science and Technology Support Program (No. 2019JDRC0029); Zigong City Science and Technology (Nos. 2017XC16 and 2019CXRC01); Opening Project of Material Corrosion and Protection Key Laboratory of Sichuan Province (Nos. 2016CL10, 2017CL03, 2019CL05, 2018CL08, and

2018CL07); Opening Project of Sichuan Province, the Foundation of Introduced Talent of Sichuan University of Science and Engineering (Nos. 2014RC31, 2017RCL31, 2017RCL36, 2017RCL16, 2019RC05, and 2019RC07). Appreciation is also extended to Apex Nanotek Co., Ltd.

REFERENCES

1 Ahmad, J.; Bazaka, K.; Anderson, L. J.; White, R. D.; Jacob, M. V. Materials and methods for encapsulation of OPV: a review. *Renew. Sustainable. Energy. Rev.* **2013**, *27*, 104–117.
2 Lagaron, J. M.; Gimenez, E.; Catala, R.; Gavara, R. Mechanisms of moisture sorption in barrier polymers used in food packaging: amorphous polyamide vs. high-barrier ethylene-vinyl alcohol copolymer studied by vibrational spectroscopy. *Macromol. Chem. Phys.* **2003**, *204*, 704–713.
3 Tsou, C.; Yao, W.; Lu, Y. Antibacterial property and cytotoxicity of a poly(lactic acid)/nanosilver-doped multiwall carbon nanotube nanocomposite. *Polymers* **2017**, *9*, 100–113.
4 Jo, J. H.; Li, Y.; Kim, S. M.; Kim, H. E.; Koh, Y. H. Hydroxyapatite/poly (ε-caprolactone) double coating on magnesium for enhanced corrosion resistance and coating flexibility. *J. Biomater. Appl.* **2013**, *28*, 617–625.
5 Pan, W.; Yin, D. X.; Jing, H. R.; Chang, H. J.; Wen, H.; Liang, D. H. Core-corona structure formed by hyaluronic acid and poly(L-lysine) *via* kinetic path. *Chinese J. Polym. Sci.* **2019**, *37*, 36–42.
6 Zhang, K.; Li, X.; Nie, M.; Wang, Q. Helical flow-driven alignment of off-axial silver-functionalized titanium dioxide fibers in polypropylene tube suitable for medical applications. *Compos. Sci. Technol.* **2018**, *158*, 121–127.
7 Zheng, P.; Zhang, P.; Sun, Z.; Zhu, C.; An, Q. Nanostructured polyelectrolyte-surfactant complex pervaporation membranes for ethanol recovery: the relationship between the membrane structure and separation performance. *Chinese J. Polym. Sci.* **2018**, *36*, 25–33.
8 Pelto, J.; Verho, T.; Ronkainen, H.; Kaunisto, K.; Metsäjoki, J.; Seitsonen, J.; Karttunen, M. Matrix morphology and the particle dispersion in HDPE nanocomposites with enhanced wear resistance. *Polym. Test.* **2019**, *77*, 105897.
9 Tsou, C. H.; Yao, W. H.; Hung, W. S.; Suen, M. C.; de Guzman, M. R.; Chen, J.; Tsou, C. Y.; Wang, R. Y.; Chen, J. C.; Wu, C. S. Innovative plasma process of grafting methyl diallylammonium salt onto polypropylene to impart antibacterial and hydrophilic surface properties. *Ind. Eng. Chem. Res.* **2018**, *57*, 2537–2545.
10 Tsou, C. H.; Wu, C. S.; Hung, W. S.; de Guzman, M. R.; Gao, C.; Wang, R. Y.; Suen, M. C. Rendering polypropylene biocomposites antibacterial through modification with oyster shell powder. *Polymer* **2019**, *160*, 265–271.
11 Niknezhad, S.; Isayev, A. I. Online ultrasonic film casting of LLDPE and LLDPE/clay nanocomposites. *J. Appl. Polym. Sci.* **2013**, *129*, 263–275.
12 Alebooyeh, R.; MohammadiNafchi, A.; Jokr, M. The effects of ZnO nanorods on the characteristics of sago starch biodegradable films. *J. Chem. Health. Risks* **2012**, *2*, 13–16.
13 Arfat, Y. A.; Benjakul, S.; Prodpran, T.; Sumpavapol, P.; Songtipya, P. Physicomechanical characterization and antimicrobial properties of fish protein isolate/fish skin gelatin-zinc oxide (ZnO) nanocomposite films. *Food Bioprocess. Technol.* **2016**, *9*, 101–112.
14 Novoselov, K. S.; Geim, A. K.; Morozov, S. V.; Jiang, D.; Zhang, Y.; Dubonos, S. V.; Grigorieva, I. V.; Firsov, A. A. Electric field effect in atomically thin carbon films. *Science* **2004**, *306*, 666–669.
15 He, F.; Fan, J.; Ma, D.; Zhang, L.; Leung, C.; Chan, H. L. The attachment of FeO nanoparticles to graphene oxide by covalent bonding. *Carbon* **2010**, *48*, 3139–3144.
16 He, F.; Lam, K. H.; Fan, J.; Chan, L. H. Improved dielectric properties for chemically functionalized exfoliated graphite nanoplates/syndiotactic polystyrene composites prepared by a solution-blending method. *Carbon* **2014**, *80*, 496–503.
17 Girdthep, S.; Sankong, W.; Pongmalee, A.; Saelee, T.; Punyodom, W.; Meepowpan, P.; Worajittiphon, P. Enhanced crystallization, thermal properties, and hydrolysis resistance of poly(lactic acid) and its stereocomplex by incorporation of graphene nanoplatelets. *Polym. Test.* **2017**, *61*, 229–239.
18 Lau, K. Y.; Ker, P. J.; Abas, A. F.; Alresheedi, M. T.; Mahdi, M. A. Long-term stability and sustainability evaluation for mode-locked fiber laser with graphene/PMMA saturable absorbers. *Opt. Commun.* **2019**, *435*, 251–254.
19 Roshan, M. J.; Jeevika, A.; Bhattacharyya, A.; Shankaran, D. R. One-pot fabrication and characterization of graphene/PMMA composite flexible films. *Mater. Res. Bull.* **2018**, *105*, 133–141.
20 Kashyap, S.; Pratihar, S. K.; Behera, S. K. Strong and ductile graphene oxide reinforced PVA nanocomposites. *J. Alloys. Compd.* **2016**, *684*, 254–260.
21 Shao, L.; Li, J.; Guang, Y.; Zhang, Y.; Zhang, H.; Che, X.; Wang, Y. PVA/polyethyleneimine-functionalized graphene composites with optimized properties. *Mater. Des.* **2016**, *99*, 235–242.
22 Elashmawi, I. S.; Alatawi, N. S.; Elsayed, N. H. Preparation and characterization of polymer nanocomposites based on PVDF/PVC doped with graphene nanoparticles. *Results. Phys.* **2017**, *7*, 636–640.
23 Hasan, M.; Lee, M. Enhancement of the thermo-mechanical properties and efficacy of mixing technique in the preparation of graphene/PVC nanocomposites compared to carbon nanotubes/PVC. *Prog. Nat. Sci: Mater. Int.* **2014**, *24*, 579–587.
24 Babaahmadi, V.; Montazer, M.; Gao, W. Low temperature welding of graphene on PET with silver nanoparticles producing higher durable electro-conductive fabric. *Carbon* **2017**, *118*, 443–451.
25 Cao, X.; Liu, X.; Li, X.; Lei, X.; Chen, W. Conductive stability of graphene on PET and glass substrates under blue light irradiation. *Opt. Commun.* **2018**, *406*, 169–172.
26 Koutsoumpis, S.; Klonos, P.; Raftopoulos, K. N.; Papadakis, C. M.; Bikiaris, D.; Pissis, P. Morphology, thermal properties and molecular dynamics of syndiotactic polystyrene (*s*-PS) nanocomposites with aligned graphene oxide and graphene nanosheets. *Polymer* **2018**, *153*, 548–557.
27 Mistretta, M. C.; Botta, L.; Vinci, A. D.; Ceraulo, M.; La Mantia, F. P. Photo-oxidation of polypropylene/graphene nanoplatelets composites. *Polym. Degrad. Stab.* **2019**, *160*, 35–43.
28 Li, C. Q.; Zha, J. W.; Long, H. Q.; Wang, S. J.; Zhang, D. L.; Dang, Z. M. Mechanical and dielectric properties of graphene incorporated polypropylene nanocomposites using polypropylene-graft-maleic anhydride as a compatibilizer. *Compos. Sci. Technol.* **2017**, *153*, 111–118.
29 La Mantia, F. P.; Ceraulo, M.; Mistretta, M. C.; Botta, L. Effect of the elongational flow on morphology and properties of polypropylene/graphene nanoplatelets nanocomposites. *Polym. Test.* **2018**, *71*, 10–17.
30 Li, H.; Xie, X. M. Polyolefin-functionalized graphene oxide and its GO/HDPE nanocomposite with excellent mechanical properties. *Chin. Chem. Lett.* **2018**, *29*, 161–165.
31 Sun, C. Q.; Wang, Y.; Tay, B. K.; Li, S.; Huang, H.; Zhang, Y. B. Correlation between the melting point of a nanosolid and the cohesive energy of a surface atom. *J. Phys. Chem. B* **2002**, *106*, 10701–10705.
32 Phukan, S.; Mahanta, A.; Rashid, M. H. Size-tunable ZnO nanotapes as an efficient catalyst for oxidative chemoselective CB bond cleavage of arylboronic acids. *Appl. Catal. A* **2018**, *562*, 58–66.

https://doi.org/10.1007/s10118-020-2392-z

33 Liu, J.; Wang, Y.; Ma, J.; Peng, Y.; Wang, A. A review on bidirectional analogies between the photocatalysis and antibacterial properties of ZnO. *J. Alloys. Compd.* **2018**, *783*, 898–918.

34 Adawi, H. I.; Newbold, M. A.; Reed, J. M.; Vance, M. E.; Feitshans, I.; Bickford, L. R.; Lewinski, N. A. Nano-enabled personal care products: current developments in consumer safety. *NanoImpact* **2018**, *11*, 170–179.

35 Newman, M. D.; Stotland, M.; Ellis, J. I. The safety of nanosized particles in titanium dioxide- and zinc oxide-based sunscreens. *J. Am. Acad. Dermatol.* **2009**, *61*, 690–692.

36 Kumar, K.; Shyamlal, B. R. K.; Gupta, A.; Mathur, M.; Swami, A. K.; Chaudhary, S. Efficacious fungicidal potential of composite derived from nano-aggregates of Cu-Diclofenac complexes and ZnO nanoparticles. *Compos. Commun.* **2018**, *10*, 81–88.

37 Guo, W.; Xue, X.; Wang, S.; Lin, C.; Wang, Z. L. An integrated power pack of dye-sensitized solar cell and Li battery based on double-sided TiO_2 nanotube arrays. *Nano Lett.* **2012**, *12*, 2520–2523.

38 Look, D. C. Recent advances in ZnO materials and devices. *Mater. Sci. Eng. B* **2001**, *80*, 383–387.

39 Ozgur, U.; Alivov, Y. I.; Liu, C.; Teke, A.; Reshchikov, M.; Doğan, S.; Morkoç, H. A comprehensive review of ZnO materials and devices. *J. Appl. Phys.* **2005**, *98*, 41301–41310.

40 Wang, L.; Zheng, Y.; Li, X.; Dong, W.; Tang, W.; Chen, B.; Xu, W. Nanostructured porous ZnO film with enhanced photocatalytic activity. *Thin Solid Films* **2011**, *519*, 5673–5678.

41 Zhang, L.; Jian, Y.; Ding, Y.; Povey, M.; York, D. Investigation into the antibacterial behaviour of suspensions of ZnO nanoparticles (ZnO nanofluids). *J. Nanoparticle Res.* **2007**, *9*, 479–489.

42 Janaki, A. C.; Sailatha, E.; Gunasekaran, S. Synthesis, characteristics and antimicrobial activity of ZnO nanoparticles. *Spectrochim. Acta Part A* **2015**, *144*, 17–22.

43 Yang, X. J.; Shi, C. S.; Xu, X. L. Studies and development of nano-ZnO. *J. Inorg. Polym. Mater.* **2003**, *18*, 1–10.

44 Tarani, E.; Terzopoulou, Z.; Bikiaris, D. N.; Kyratsi, T.; Chrissafis, K.; Vourlias, G. Thermal conductivity and degradation behavior of HDPE/graphene nanocomposites. *J. Therm. Anal. Calorim.* **2017**, *129*, 1715–1726.

45 Mwafy, E. A.; Abd-Elmgeed, A. A.; Kandil, A. A.; Elsabbagh, I. A.; Elfass, M. M.; Gaafar, M. S. High UV-shielding performance of zinc oxide/high-density polyethylene nanocomposites. *Spectrosc. Lett.* **2015**, *48*, 646–652.

46 Tang, W.; Santare, M. H.; Advani, S. G. Melt processing and mechanical property characterization of multi-walled carbon nanotube/high density polyethylene (MWNT/HDPE) composite films. *Carbon* **2003**, *41*, 2779–2785.

47 Li, S. C.; Li, Y. N. Mechanical and antibacterial properties of modified nano-ZnO/high-density polyethylene composite films with a low doped content of nano-ZnO. *J. Appl. Polym. Sci.* **2010**, *116*, 2965–2969.

https://doi.org/10.1007/s10118-020-2392-z